JOURNAL OF THERMOPHYSICS AND HEAT TRANSFER
Vol. 22, No. 3, July–September 2008

Recombination-Assisted Nitrogen Dissociation Rates Under Nonequilibrium Conditions

Gianpiero Colonna* and Lucia Daniela Pietanza†
Consiglio Nazionale Delle Ricerche, 70126 Bari, Italy
and
Mario Capitelli‡
Università di Bari, 70126 Bari, Italy

DOI: 10.2514/1.33505

A macroscopic kinetic model accounting for non-Boltzmann vibrational distributions is proposed to describe the dissociation kinetics of a N_2/N mixture in a recombination regime. This model is derived by reducing the state-to-state approach to a kinetic equation describing the last vibrational level. The global dissociation rates are related to the last vibrational level population instead of the vibrational temperature. Results obtained by this model were validated with state-to-state calculations.

Nomenclature

E_{vib}	=	function to calculate the energy of the vth vibrational state
G_v	=	global gain term for the vth vibrational level
G_v^p	=	gain term for the vth vibrational level due to pth process
G_v^*	=	approximated global gain term for the vth vibrational level
K_{eq}	=	equilibrium constant for the dissociation process
K^d	=	generic dissociation rates
K_v^{da}	=	rates for dissociation from vth level induced by atomic collisions
K_v^{dm}	=	rates for dissociation from vth level induced by molecular collisions
K^r	=	generic recombination rates
K_v^{ra}	=	rates for recombination in vth level induced by atomic collisions
K_v^{rm}	=	rates for recombination in vth level induced by molecular collisions
$K_{v,w}^{vT}$	=	rates for vT transition $v \rightarrow w$
$K_{v,w}^{vv}$	=	rates for vv transitions $v, w-1 \rightarrow v-1$, and w
$K_{v,w}^{X}$	=	state-to-state rate of the process X for the molecular transition $v \rightarrow w$
K^{xa}	=	rate coefficients of process x induced by atoms
K^{xm}	=	rate coefficients of process x induced by molecules
k	=	Boltzmann constant
L_v	=	global loss term for the vth vibrational level
L_v^p	=	loss term for the vth vibrational level due to the pth process
L_v^*	=	approximated global loss term for the vth vibrational level
N_{lev}	=	number of vibrational levels
N_{tot}	=	total particle density of the mixture
N_v	=	particle density of the vth vibrational state
n_v	=	vibrational distribution
Q_{vib}	=	vibrational partition function
R^x	=	global rate coefficient for the x process
T	=	gas temperature
T_v	=	vibrational temperature
t	=	time
γ	=	ratio between constant pressure and constant volume specific heat
ε_v	=	energy of the vth vibrational state
ε_{vib}	=	mean vibrational energy
χX	=	molar fraction of the Xth species

Subscripts

v	=	vibrational quantum number
vM	=	last vibrational level
w	=	vibrational quantum number

I. Introduction

ACCURATE characterization of high-enthalpy flows strongly depends on the nonequilibrium vibrational distributions present in the medium. Two approaches are currently used for handling the problem: multitemperature (MT) and state–to–state (STS) models. The MT approach considers Boltzmann vibrational distribution, characterized as a vibrational temperature that is different from the translational temperature. For diatomic molecules, the common assumption is to consider the rotational degree of freedom in equilibrium with the gas, whereas a linear relaxation equation is considered for the vibrational temperature [1,2]. The relevant role of the vibrational temperature is to affect the rate coefficients for chemical reactions, such as molecular dissociation, considering that endothermic processes are accelerated by vibrationally excited molecules. According to Park's model [3–5], Arrhenius rates for the relevant processes are calculated by introducing an effective temperature, defined as the geometrical mean of the translational and vibrational temperatures [3–5]. This approach, which is very popular due to its simple implementation in 2-D and 3-D fluid dynamics codes, adequately describes the dissociation regime, but it is not accurate in the recombination regime.

In the last years, a new model based on the STS vibrational kinetics has been developed and applied to 1-D high-enthalpy flows, such as boundary layer [6,7], nozzle expansion [8–10], and shock wave [8,11]. This model predicts long plateaus in the vibrational distributions generated by the preferential pumping of high-lying vibrational

Presented as Paper 4554 at the 39th AIAA Thermophysics Conference, Miami, FL, 25–28 June 2007; received 17 July 2007; revision received 3 March 2008; accepted for publication 6 March 2008.

*Ph.D., Senior Researcher, Istituto di Metodologie Inorganiche e dei Plasmi, Via Amendola 122-D; gianpiero.colonna@ba.imip.cnr.it. Member AIAA.

†Ph.D., Researcher, Istituto di Metodologie Inorganiche e dei Plasmi; daniela.pietanza@ba.imip.cnr.it

‡Full Professor, Dipartimento di Chimica; mario.capitelli@ba.imip.cnr.it. Fellow AIAA.

levels due to the recombination process. As a consequence, global chemical rates do not follow the Arrhenius trend and are related to the atom concentration rather than to the vibrational temperature [12].

Implementation of STS kinetics in 2-D and 3-D codes dramatically increases the computational time so that researchers are trying to develop macroscopic models that include the main features of the state–to–state approach. The first attempts to define such models [13–17] introduce a correction factor to the Park model [3–5], taking into account the departure of the distribution tails from the Boltzmann behavior. These models work well in dissociation regimes (shock waves) but are not adequate to describe nozzle flows, where recombination is dominant.

In a previous work [12], the behavior of vibrational distributions and rates in dissociation and recombination regimes was discussed. The main result of this study is that the dissociation rates in the recombination regime are related to atomic concentration rather than to vibrational temperature. Approximate analytical solutions of the kinetic problem (both in dissociation and recombination regimes) were also presented, providing a qualitative description of the relevant rates. A fitting function of the rates that depend on the gas temperature and dissociation degree was proposed, showing a qualitative agreement with the state-to-state calculations.

In the present paper, the state-to-state kinetic model was improved with respect to that used in [12] and a new macroscopic kinetic model, reproducing STS kinetic features in the recombination regime, is proposed and applied to study the kinetics of a N_2/N mixture.

II. Model Description

A. State-to-State Kinetics

The STS model considered in the present work includes two species, N_2 and N, both in the electronic ground state. The whole vibrational ladder of nitrogen molecule is considered, and rotation is in equilibrium with the gas temperature ($\gamma = \frac{7}{5}$). In particular, we consider 67 vibrational levels, in agreement with the potential energy surface used in the quasi-classical trajectory (QCT) calculations of Esposito and Capitelli [18] (see also [6,10,19]).

The energy of the vibrational levels is calculated using the equations [20]

$$\begin{aligned} \varepsilon_v &= E_{\text{vib}}(v+\tfrac{1}{2}) - E_{\text{vib}}(\tfrac{1}{2}) \\ E_{\text{vib}}(\xi) &= \omega_e\xi - \omega_e x_e\xi^2 + \omega_e y_e\xi^3 + \omega_e z_e\xi^4 \end{aligned} \tag{1}$$

where the coefficients ω_e, $\omega_e x_e$, $\omega_e y_e$, and $\omega_e z_e$ are given in the New column in Table 1.

State-to-state kinetics include the following processes:

For vTm:

$$\mathrm{N}_2(v) + \mathrm{N}_2 \rightleftharpoons \mathrm{N}_2(v-1) + \mathrm{N}_2$$

For vTa:

$$\mathrm{N}_2(v) + \mathrm{N} \rightleftharpoons \mathrm{N}_2(v-\Delta v) + \mathrm{N}$$

For vv:

$$\mathrm{N}_2(v) + \mathrm{N}_2(w-1) \rightleftharpoons \mathrm{N}_2(v-1) + \mathrm{N}_2(w)$$

For drm:

$$\mathrm{N}_2(v) + \mathrm{N}_2 \rightleftharpoons 2\mathrm{N} + \mathrm{N}_2$$

Table 1 Coefficients for Eq. (1) used in this paper (new) and those used for correlation of N_2–N_2 rates (old).

Coefficient	New [10]	Old [6]
ω_e	2.3724463054×10^3	2.35857×10^3
$\omega_e x_e$	1.81016777×10^1	1.4324×10^1
$\omega_e y_e$	$1.2755162435 \times 10^{-2}$	-2.26×10^{-2}
$\omega_e z_e$	$-7.9594872485 \times 10^{-5}$	0.0

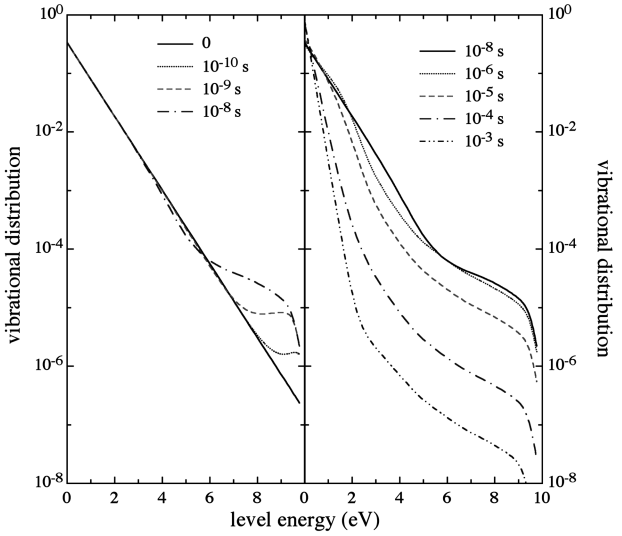

Fig. 1 Relaxation of the vibrational distribution for the initial conditions $Tv0 = 8000$ K, $T = 2000$ K, and $\chi_N = 0.9$.

For dra:

$$\mathrm{N}_2(v) + \mathrm{N} \rightleftharpoons 2\mathrm{N} + \mathrm{N}$$

The rates of molecule–molecule (vTm and vv) collisions were obtained [21] considering the Herzberg-level scheme [6,20] ($N_{\text{lev}} = 47$). The coefficients for Eq. (1) are reported in the Old column in Table 1. Under the assumption that the rates are related to the level energy rather than to the vibrational quantum number, the value v' to be used in the rate expression must be related to the vibrational quantum number v in the considered level scheme, solving the equation

$$E_{\text{vib}}^{\text{old}}(v'+\tfrac{1}{2}) - E_{\text{vib}}^{\text{old}}(\tfrac{1}{2}) = E_{\text{vib}}^{\text{new}}(v+\tfrac{1}{2}) - E_{\text{vib}}^{\text{new}}(\tfrac{1}{2}) \tag{2}$$

where the superscripts new and old refer to the coefficient set in Table 1.

For vTm collisions, the rate coefficient data were taken from [21] and fitted with the function

$$\begin{aligned} &\ln K_{v,v-1}^{vTm} = k_0(\ln v) + a_1(\ln v) + \sigma[\ln T, c_1(\ln v), \delta_1(\ln v)] \\ &\quad + a_2(\ln v) + \sigma[\ln T, c_2(\ln v), \delta_2(\ln v)] \\ &\text{coef}_i(\xi) = \alpha_0 + (\alpha_1 \cdot \xi) + \alpha_2 \cdot [\exp(\alpha_3 \cdot \xi) - 1] + \alpha_4 \cdot \xi^2 \\ &\text{coef}_i \equiv k_0, a_i, c_i, \delta_i \\ &\sigma(x,c,\delta) = \frac{\exp(-(x-c)/\delta)}{\exp(-(x-c)/\delta) + \exp((x-c)/\delta)} \end{aligned} \tag{3}$$

where the coefficients α_j are reported in Table 2. The data in [21] were available in the range 200–8000 K, but extrapolation is possible due to the long-range behaviors of function (3). It must be noted that the vibrational quantum number to be used in this expression must be v', obtained from Eq. (2).

The rate coefficients for vv processes are those used in [6]. As for vTm, the vibrational quantum numbers to be used in the rate expression must be the solution of Eq. (2). QCT calculations [18,22] refined in [23] were used for vTa rates. These data are more accurate than those used in [10,24], because of the increasing number of trajectories in QCT calculations.

The dissociation-recombination models were considerably improved with respect to [12], in which the ladder-climbing (LC) model [6,7,9,12] was used. The LC model, extending the internal transition rates to a virtual level above the dissociation limit, underestimates dissociation rates up to 2 orders of magnitude [10,24]. For the dra process, QCT rates [10,18,22–24] were used. For molecule–molecule dissociation drm, no state-to-state data set is available. Instead of using the LC approach, the same dependence

Table 2 Coefficients for *vTm* rate fittings in Eq. (3)

Coefficient	α_0	α_1	α_2	α_3	α_4
k_0	−23.45450	−42.53388	2520.085	1.706869×10^{-2}	−0.3185535
a_1	−22.86601	−0.5830948	1.257130×10^{-7}	4.065968	0
c_1	7.460484	−0.1121130	-8.053625×10^{-3}	1.422084	0
δ_1	−1.643407	7.533923×10^{-3}	-8.921238×10^{-3}	1.278885	0
a_2	−5.312718	−0.5391023	2.583197	0.3241316	0
c_2	6.191806	2.500253×10^{-4}	92.27724	-1.217381×10^{-3}	6.588638
δ_1	−0.5650175	8.912830×10^{-3}	0	0	0

from T and v as dra was considered for drm rates, normalized to the thermal molecule–molecule dissociation rate proposed by Chernyi et al. [25] which considers the following relation between thermal dra and drm rates [23]

$$\frac{K_v^{rm}(T)}{K_v^{ra}(T)} = \frac{K_v^{dm}(T)}{K_v^{da}(T)} = 0.1694 + 5.5249 \times 10^{-5} T + 5.2927 \times 10^{-9} 2.2742 \times 10^{-13} \tag{4}$$

For vT and vv processes, only exothermal rates are given, and for endothermic processes, the rate coefficients are calculated applying the detailed balance principle:

$$K_{w,v}^{vT}(T) = K_{v,w}^{vT}(T) \exp\left(-\frac{\varepsilon_v - \varepsilon_w}{kT}\right) \tag{5}$$

$$K_{w,v}^{vv}(T) = K_{v,w}^{vv}(T) \exp\left(-\frac{\varepsilon_v - \varepsilon_{v-1} + \varepsilon_{w-1} - \varepsilon_w}{kT}\right) \tag{6}$$

To calculate the recombination rates, the detailed balance principle has also been applied in the form

$$K_v^r(T) = K_v^d(T) \frac{\exp[-(\varepsilon_v/kT)]}{Q_{\text{vib}}(T) K_{\text{eq}}(T)} \tag{7}$$

where the equilibrium constant for N_2 dissociation (in pascals) is given by

$$\ell_n K_{\text{eq}} = 20.802708 - 113.80656\left(\frac{1000}{T}\right)^{0.998746} + 0.133550 \exp\left(\frac{T}{-8430.0834}\right) + 0.755434\, \ell_n(T) \tag{8}$$

Knowing the vibrational distribution, it is possible to evaluate the mean vibrational energy,

$$\varepsilon_{\text{vib}} = \sum_{v=0}^{N_{\text{lev}}} \varepsilon_v n_v \tag{9}$$

the vibrational temperature from the population of the first two levels,

$$T_v = \frac{\varepsilon_1 - \varepsilon_0}{k\, \ell_n(n_0/n_1)} \tag{10}$$

and the global dissociation and recombination rate coefficients:

$$R^d(T, n_v) = \sum_{v=0}^{N_{\text{lev}}} K_v^d(T) n_v \qquad R^r(T) = \sum_{v=0}^{N_{\text{lev}}} K_v^r(T) \tag{11}$$

B. Multitemperature Model

The MT macroscopic model was constructed to be consistent with the state-to-state kinetics. The vibrational energy, calculated by summing the Boltzmann distribution over the considered levels [see Eq. (1)], evolves following the relaxation equation as in [3]. On the other hand, the dissociation rates $R^d(T, T_v)$ were obtained from the STS model by summing the state-selected rates over a Boltzmann vibrational distribution [see Eq. (11)] at the vibrational temperature T_v. The global recombination rates are calculated by applying the detailed balance to the thermal dissociation $R^d(T, T)$, considering the recombination process to be independent of the vibrational distribution.

C. Two-Level Distribution Kinetics

Coupling state-to-state kinetic model in fluid dynamics codes considerably increases the computational load, making such an approach difficult, but not impossible, for application in 2-D and 3-D calculations. On the other hand, the MT approach, which requires lower computational times, cannot reproduce the behavior of global rates predicted by STS calculations [9,12]. The state-to-state model predicts a fast relaxation of the distribution tails to a quasi-stationary value (see Fig. 1, left plot), whereas the low-energy distribution does not change. For longer times, the vibrational temperature starts decreasing, due to vT collisions, as well as the distribution tails, following the variation of atomic concentration. The global rates are strongly related to the distribution tails, as discussed in [9,12].

The feasibility of a macroscopic model that accounts for nonequilibrium distributions has been investigated in [12], in which the global dissociation rates were reported as a function of atomic concentration (see Fig. 2). This approach does not predict the short-time behavior of the rates (see Figs. 2 and 3), whereas the global

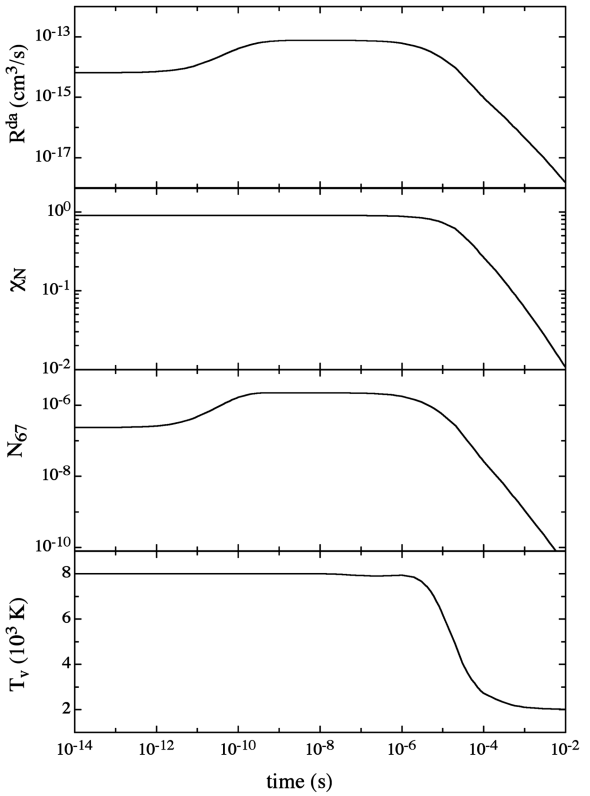

Fig. 2 Time profiles of $N_2 + N$ dissociation rates, atomic molar fraction, population of the last level, and vibrational temperature for initial conditions $Tv0 = 8000$ K, $T = 2000$ K and $\chi_N = 0.9$.

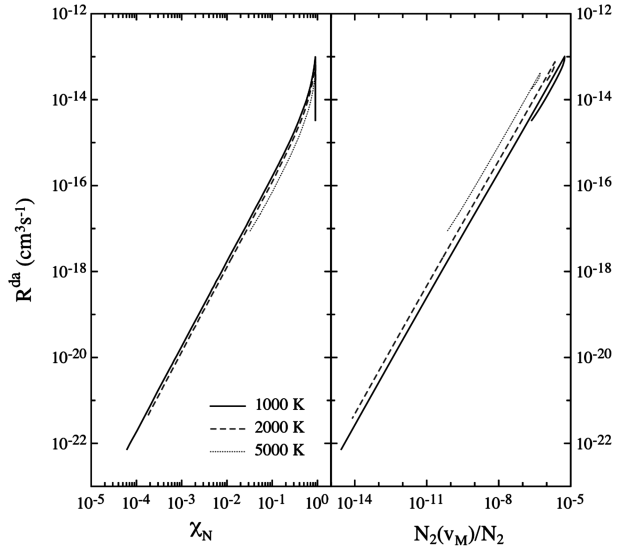

Fig. 3 $N_2 + N$ global dissociation rates in the state-to-state kinetics as a function of atomic molar fraction (left) and of the last level population (right) for initial conditions $Tv0 = 8000$ K and $\chi_N = 0.9$.

dissociation rates closely follow the trend of the population of the last vibrational level. Moreover, this model can be applied when recombination is the dominant process [12], whereas close to equilibrium or in the dissociation regime, it is not adequate.

As observed in Fig. 3, there is a linear relation between the logarithm of the dissociation rates calculated with the state-to-state model and the fraction of molecules in the last vibrational level. Using 0-D kinetics, the time evolution of the vibrational distribution, molar fraction, and the global dissociation rates were calculated at constant pressure and temperature for different gas temperatures in the range of 50–5000 K, considering $\chi_N = 0.9$ and $T_v = 8000$ K as the initial conditions. These results were fitted by the equation

$$\ell n\, R^d(T, n_{v_M}) = a(\ell n\, T) + b(\ell n\, T)\, \ell n(n_{v_M}) \tag{12}$$

where a and b are polynomial functions of $\ell n\, T$,

$$\left.\begin{matrix} a(x) \\ b(x) \end{matrix}\right\} = \sum_{i=0}^{5} \alpha_i x^i \tag{13}$$

and the α_i values are reported in Table 3. Initial conditions influence only the short-time behavior, in which the small departures from the fitting functions are determined by the relaxation of the distribution tails to the quasi-steady-state values. It must be noted, however, that the error is much smaller if the rates are related to the last vibrational level rather than to the atomic molar fraction (see Fig. 3). A comparison of results reported in Figs. 2 and 3 shows that the two-level distribution (TLD) rates deviate from the linear trend for $t < 10^{-9}$, a time scale too short for fluid dynamics characteristic times. Moreover, it has been shown [12] that the quasi-steady-state solution does not depend on the initial vibrational temperature, but only on the atomic molar fraction and gas temperature. It is worth noticing that the global rates, even if calculated by considering multiquantum transitions, depend only on the last vibrational level population because it is strongly correlated to all the other high-lying levels.

This characteristic is the key point of the TLD model. It consists of describing the vibrational distribution with two quantities: the vibrational energy, as in the multitemperature model, representing the low-lying vibrational states, and the population of the last vibrational level, representing the distribution tail, to determine the dissociation rates.

The vibrational-energy relaxation can be investigated using the same equation as in the multitemperature model, whereas the time evolution of the last vibrational level should be based on the state-to-state model. Consider, for example, the contribution of the vTm processes:

$$\frac{dN_v}{dt} = N_{tot}\chi_{N_2}(K^{vTm}_{v+1,v}N_{v+1} + K^{vTm}_{v-1,v}N_{v-1}) - N_{tot}\chi_{N_2}(K^{vTm}_{v,v-1} + K^{vTm}_{v,v+1})N_v \tag{14}$$

Other processes contribute with similar terms. The general expression of the kinetic equation for a given vibrational level can be written as the difference of the gain G_v and loss L_v terms:

$$\frac{dN_v}{dt} = G_v - L_v N_v \tag{15}$$

which includes the contribution of all the considered processes (vTm, vTa, drm, dra, and vv):

$$\begin{aligned} G_v &= G_v^{vTm} + G_v^{vTa} + G_v^{ra} + G_v^{rm} + G_v^{vv} \\ L_v &= L_v^{vTm} + L_v^{vTa} + L_v^{ra} + L_v^{dm} + L_v^{vv} \end{aligned} \tag{16}$$

The gain terms are given by

$$G_v^{vTm} = N_{tot}\chi_{N_2} \sum_{\substack{w=0 \\ v \neq w}}^{N_{lev}} K^{vTm}_{w,v} N_w \tag{17}$$

$$G_v^{vTa} = N_{tot}\chi_{N} \sum_{\substack{w=0 \\ v \neq w}}^{N_{lev}} K^{vTa}_{w,v} N_w \tag{18}$$

$$G_v^{rm} = N_{tot}^3 \chi_N^2 \chi_{N_2} K_v^{rm} \tag{19}$$

$$G_v^{ra} = N_{tot}^3 \chi_N^3 K_v^{ra} \tag{20}$$

$$G_v^{vv} = \sum_{\substack{w=1 \\ v \neq w}}^{N_{lev}} (K^{vv}_{w,v} N_{v-1} N_w + K^{vv}_{v+1,w} N_{v+1} N_{w-1}) \tag{21}$$

and the loss terms are given by

$$L_v^{vTm} = N_{tot}\chi_{N_2} \sum_{\substack{w=0 \\ v \neq w}}^{N_{lev}} K^{vTm}_{v,w} \tag{22}$$

Table 3 Coefficients of the polynomials to calculate a and b in Eq. (13) for the dissociation rates by molecules and atoms

Rate	Coeff.	α_0	α_1	α_2	α_3	α_4	α_5
	a	37.9849	−48.89864	16.48396	−2.7588870	0.2292134	−0.007487
R^{da}	b	3.714972	−2.584976	0.9610557	−0.1737152	0.015209	−0.0005165
	a	−127.2788	67.80164	−16.46543	1.838103	−0.0875159	0.001146
R^{dm}	b	4.086736	−2.892419	1.060681	−0.1895913	0.0164573	−0.0005553

$$L_v^{vTa} = N_{\text{tot}}\chi_{\text{N}} \sum_{\substack{w=0 \\ v \neq w}}^{N_{\text{lev}}} K_{v,w}^{vTa} \tag{23}$$

$$L_v^{dm} = N_{\text{tot}}\chi_{\text{N}}^2\chi_{\text{N}_2}K_v^{dm} \tag{24}$$

$$L_v^{dm} = N_{\text{tot}}\chi_N^3 K_v^{da} \tag{25}$$

$$L_v^{vv} = \sum_{\substack{w=1 \\ v \neq w}}^{N_{\text{lev}}} (K_{w,v+1}^{vv}N_w + K_{v,w}^{vv}N_{w-1}) \tag{26}$$

the ratio between the gains due to recombination and the neglected gain terms (vT up-pumping and vv). Three relevant aspects emerge:

1) The dissociation process is also relevant in the recombination regime, due to nonequilibrium distributions.

2) Transitional and quasi-stationary STS solutions are accurately described by Eq. (27).

3) The error made using the approximated value G_v^* does not exceed a few percent.

This model can be used to directly determine the value of the last level population and the dissociation rates if quasi-steady-state approximation is valid. There is some evidence (see [12]) that in some fluid dynamics conditions (boundary layer [6,7]), due to the rapid change in external conditions P and T, the quasi-steady-state conditions are not reached. As a consequence, the numerical solution of Eq. (15) must be calculated.

In conclusion, the system of master equations to be solved in the TLD approach is

$$\begin{cases} \frac{\mathrm{d}N_{\text{N}_2}}{\mathrm{d}t} = R^{rm}(T)N_{\text{N}_2}N_{\text{N}}^2 + R^{ra}(T)N_{\text{N}}^3 - R^{dM}(T, n_{v_M})N_{\text{N}_2}^2 - R^{da}(T, n_{v_M})N_{\text{N}_2}N_{\text{N}} \\ \frac{\mathrm{d}N_{\text{N}}}{\mathrm{d}t} = 2[R^{dm}(T, n_{v_M})N_{\text{N}_2}^2 + R^{da}(T, n_{v_M})N_{\text{N}_2}N_{\text{N}} - R^{rm}(T)N_{\text{N}_2}N_{\text{N}}^2 - R^{\text{ra}}(T)N_{\text{N}}^3] \\ \frac{\mathrm{d}N_{v_M}}{\mathrm{d}t} = K_{v_M}^{rm}N_{\text{N}}^2N_{\text{N}_2} + K_{v_M}^{\text{ra}}N_{\text{N}}^3 - [K_{v_M}^{dm}N_{\text{N}_2} + K_{v_M}^{da}N_{\text{N}} + \sum_{w=0}^{v_M-1}(K_{v_M,w}^{vTm}N_{\text{N}_2} + K_{v_M,v}^{vTa}N_{\text{N}})]N_{v_M} \end{cases} \tag{28}$$

Equation (15) cannot be solved only for a single level, because the gain G_v and loss L_v terms are functions of the composition and of the overall distribution.

In the recombination regime, vT up-pumping and vv collisions are negligible. This aspect has been widely discussed in the literature [6,7,9,10,12] and will be verified in the Results section. Under this approximation, the gain terms of the last vibrational level depend only on the atomic molar fraction (recombination) and not on the population of lower vibrational levels. Moreover, L_v does not depend on the distribution, being the nonlinear contribution of the neglected vv process. Therefore, Eq. (15) can be solved numerically, together with the energy and master equations, resulting in the TLD model. Under the further approximation that the composition changes slower with respect to the distribution tail (quasi-steady-state condition), G_v and L_v are constant, and therefore Eq. (15) can be solved, yielding [12]

$$N_v(t) = \left(N_v(0) - \frac{G_v^\star}{L_v^\star}\right)\exp(-L_v^\star t) + \frac{G_v^\star}{L_v^\star} \tag{27}$$

where $G_v^\star$ and $L_v^\star$ are the approximated gain and loss terms. In [12], Eq. (27) was used to qualitatively describe some behaviors of the state-to-state kinetics in the recombination regime, such as the dependence of the global dissociation rates on atomic molar fractions and the scaling law of the quasi-steady-state rates, with the pressure ($R \propto P$) being $G_v^* \propto P$ (N_{tot}) and L_v^* independent of P.

A more detailed analysis has proved that Eq. (27) is still valid if dissociation losses, neglected in [12], are also considered. The last level population obtained from Eq. (27) was compared with state-to-state calculations up to 10^{-8} s (quasi-steady-state value), giving very good agreement (see Fig. 4). The bottom plot in Fig. 4 reports

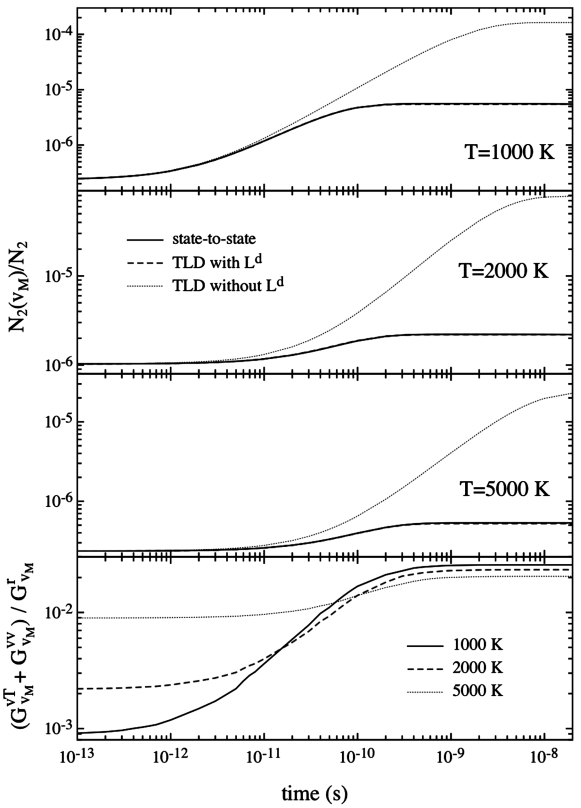

Fig. 4 Time evolution of the population of the last vibrational level at different gas temperature calculated with the state-to-state and TLD models; the relative value of vT gains is shown in the bottom frame.

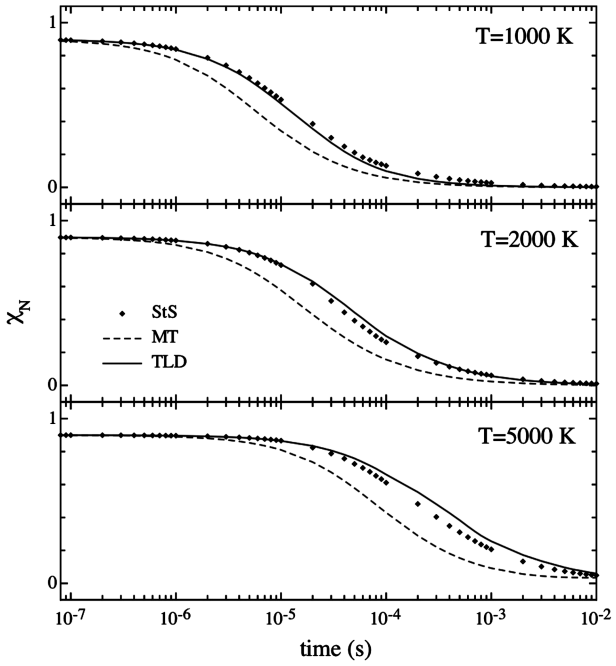

Fig. 5 Time evolution of atomic molar fraction for different gas temperatures calculated by STS, MT ($T - T_v$), and TLD for initial conditions $Tv0 = 8000$ K, $\chi_{N,0} = 0.9$, and $P = 1$ atm.

where N_{v_M} is the particle density of the molecules in the last vibrational level and $n_{v_M} = N_{v_M}/N_{N_2}$. These equations are given for a homogeneous system and can be easily transformed to the mass continuity equations for reactive flows, considering that the total density is obtained by summing the contribution of atoms and molecules, whereas the last vibrational level is considered only to calculate the rate coefficient of $n_{v_M} = \rho_{v_M}/\rho_{N_2}$.

III. Results

The first application of the TLD model [see Eq. (28)] is to determine the temporal evolution of the molar fractions of the N_2 and N species under constant pressure and temperature, with the initial conditions of a vibrational temperature higher than the gas temperature and an atomic molar fraction higher than the equilibrium value (recombination regime).

In Fig. 5, the time evolution of the molar fraction of atomic nitrogen χ_N calculated with the state-to-state model was compared with the corresponding values obtained by MT and TLD macroscopic models for different gas temperatures. State-to-state and TLD results are in good agreement, whereas the multitemperature model predicts lower values for the atomic molar fraction. This is due to the fact that the multitemperature model underestimates the vibrational distribution tails, resulting in smaller dissociation rates and faster recombination kinetics. On the other hand, the agreement between the STS and TLD models is rather good, implying that the TLD approach reproduces the main properties of STS calculations. Some differences can be observed between STS and TLD calculations when the atomic concentration decreases, approaching local equilibrium. This result can be expected, because the TLD model is valid in the recombination regime. The analysis of the factors that determine the differences between the two models can help to extend the range of validity of the TLD approach. These discrepancies can be attributed to two factors: errors between the global rate and the fitting function [see Eqs. (12) and (13)] and the contribution of the neglected gain terms in Eq. (15).

The first error source can be due to loss of correlation between the global dissociation rates and the last vibrational level population. This contribution does not exceed a small percentage, as can be observed in Fig. 6, in which the rate coefficients for the $N_2 + N$ dissociation process used in TLD calculations are compared with state-to-state results. The largest differences are observed for high

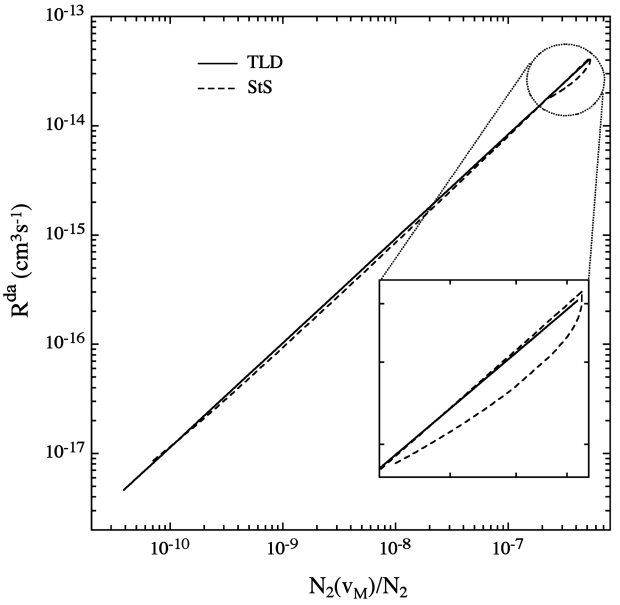

Fig. 6 Comparison of the rate coefficient of the $N_2 + N$ dissociation collisions calculated with the state-to-state and TLD models for $T = 5000$ K in the same conditions as in Fig. 5.

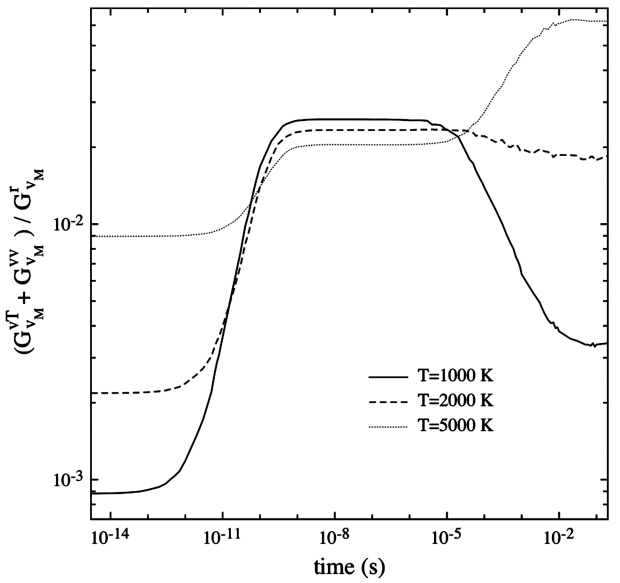

Fig. 7 Contribution of the neglected gain terms [$G^{vTm}_{v_M}$, $G^{vTa}_{v_M}$, and $G^{vv}_{v_M}$ in Eqs. (17), (18), and (21)] relative to the recombination gains [$G^{rm}_{v_M}$ and $G^{ra}_{v_M}$ in Eqs. (19) and (20)] for different gas temperatures.

atomic concentrations (see the magnified frame in Fig. 6). This happens during the relaxation phase, when the distribution tail is adapting to the quasi-steady-state solution.

The other source of inaccuracy is neglecting vT up-pumping [$G^{vTa}_{v_M}$ and $G^{vTm}_{v_M}$ in Eqs. (17) and (18)] and vv [$G^{vv}_{v_M}$ in Eq. (21)] terms in the TLD model. The relative contribution of the neglected gain terms was investigated by solving the complete state-to-state kinetic equations and is reported in Fig. 7. This contributions do not exceed 10% of the recombination terms, the maximum value occurring for the highest considered temperature ($T = 5000$ K) and for $t > 10^{-2}$ s.

To better understand the approximations made in the TLD model, STS calculations are performed by considering similar assumptions as in TLD, in conditions in which the discrepancy is larger ($T = 5000$ K), and are compared with the exact STS results (see Fig. 8). We can note that the contribution of vv processes is completely negligible under the recombination regime, as described

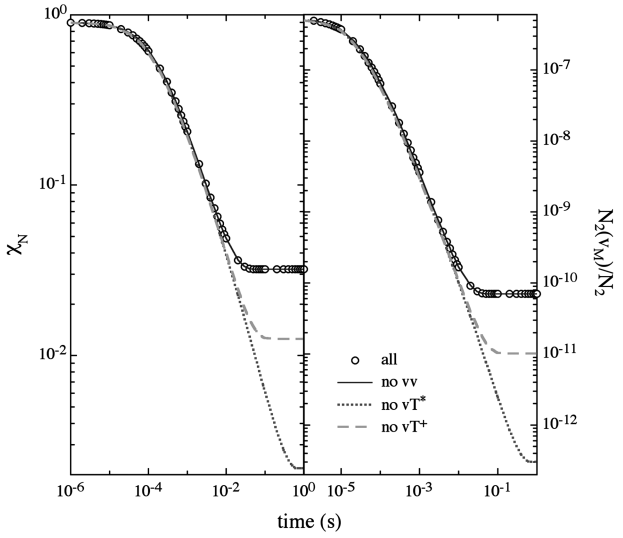

Fig. 8 Comparison between different STS calculations: exact solution (all), neglecting *vv* collisions (no *vv*), neglecting *vv* and *vT* up-pumping (no *vT), and neglecting *vv* and *vT* up-pumping only for $v \geq 20$ (no vT^+).**

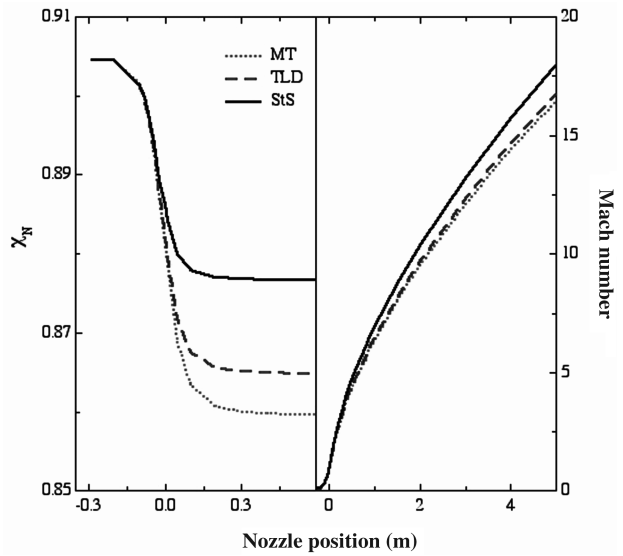

Fig. 9 Atomic nitrogen and Mach number profiles for F4 nozzle expansion [9] calculated with STS, TLD, and MT models for stagnation conditions $T = 8000$ K and $P = 1$ atm; the origin of the x axis corresponds to the nozzle throat; the inlet is at $x = -0.3$ m and the exit is at $x = 4.0$ m.

in [12]. The other considered approximation consists of neglecting the vT up-pumping from all levels (* case in Fig. 8) or from high-lying levels (+ case in Fig. 8). Both assumptions are not important for $t < 10^{-2}$ s, yielding different results approaching the equilibrium state, however, in which the detailed balance principle fails.

The TLD model was implemented in 1-D nozzle expansion numerical code. It must be stressed that the TLD rates reported in Eq. (12) do not verify the detailed balance principle and that this model fails at equilibrium (i.e., at the nozzle inlet). To overcome this problem, the TLD rates must be modified to extend its applicability in the whole nozzle flowfield. For this purpose, the following expression for the dissociation rates was proposed:

$$R(T, T_v, n_{v_M}) = R^{\mathrm{MT}}(T, T_v) + R^{\mathrm{TLD}}(T, n_{v_M} - n_{v_M}^{T_v}) \qquad (29)$$

where R^{MT} is the multitemperature rate, R^{TLD} is the TLD rate given in Eq. (12), and $n_{v_M}^{T_v}$ is the population of the last level for a Boltzmann distribution at T_v. In addition, for the kinetics of the last vibrational level, the detailed balance principle was enforced to make the local equilibrium a stationary solution. This model reproduces the TLD kinetics when recombination is dominant, converging toward the proper solution at equilibrium. Figure 9 compares the results obtained with the adapted TLD model with corresponding results by STS and MT. For the considered conditions, the differences are generally small; however, we note that the modified TLD slightly improves the agreement with STS calculations with respect to the MT model. The limits of the modified TLD model are a consequence of the behavior of the modified rates close to the nozzle throat, in which the *multitemperature part* of the rate in Eq. (29) dominates with respect to the TLD model, underestimating in the intermediate region the dissociation rates.

IV. Conclusions

A 0-D two-level distribution model was developed to account for the main characteristics of nonequilibrium vibrational distributions, as given by the state-to-state model under the recombination regime. The global dissociation rates were related to the population of the last vibrational level, instead of the vibrational temperature as in multitemperature models. This approach, which was also used to describe nozzle flow expansion of the N_2–N mixture, is accurate when the atomic molar fraction is larger than 10^{-2}, and the tail population is determined by the balance of recombination gains and dissociation and vT losses.

Acknowledgments

This paper was partially supported by the Agenzia Spaziale Italiana (ASI) under project Configurazioni Aerotermodinamiche Innovative per Sistemi di Trasporto Spaziale (CAST) and by Ministero dell'Istruzione, dell'Università e della Ricerca (MIUR) under the Fondo per gli Investimenti della Ricerca di Base (FIRB) Microscopic Dynamics of Chemical Reactivity project (number RBAU01H8FW).

References

[1] Treanor, C. E., and Marrone, P. V., "Effect of Dissociation on the Rate of Vibrational Relaxation," *Physics of Fluids*, Vol. 5, No. 9, 1962, pp. 1022–1026. doi:10.1063/1.1724467

[2] Marrone, P. V., and Treanor, C. E., "Chemical Relaxation with Preferential Dissociation from Excited Vibrational Levels," *Physics of Fluids*, Vol. 6, No. 9, 1963, pp. 1215–1221. doi:10.1063/1.1706888

[3] Park, C., "A Review of Reaction Rates in High Temperature Air," AIAA Paper 89-1740, 1989.

[4] Sharma, S. P., Huo, W. M., and Park, C., "Rate Parameters for Coupled Vibration-Dissociation in a Generalized SSH Approximation," *Journal of Thermophysics and Heat Transfer*, Vol. 6, No. 1, 1992, pp. 9–21.

[5] Park, C., "Review of Chemical-Kinetic Problems of Future NASA Missions, 1: Earth Entries," *Journal of Thermophysics and Heat Transfer*, Vol. 7, No. 3, 1993, pp. 385–398.

[6] Armenise, I., Capitelli, M., Colonna, G., Kudriavtsev, N., and Smetanin, V., "Nonequilibrium Vibrational Kinetics During Hypersonic Flow of a Solid Body in Nitrogen and its Influence on the Surface Heat Flux," *Plasma Chemistry and Plasma Processing*, Vol. 15, No. 3, 1995, pp. 501–528.

[7] Armenise, I., Capitelli, M., Colonna, G., and Gorse, C., "Nonequilibrium Vibrational Kinetics in the Boundary Layer of Re-Entering Bodies," *Journal of Thermophysics and Heat Transfer*, Vol. 10, No. 3, 1996, pp. 397–405.

[8] Kewley, D., "Numerical Study of Anharmonic Diatomic Relaxation Rates in Shock Waves and Nozzles," *Journal of Physics B: Atomic and Molecular Physics*, Vol. 8, No. 15, 1975, pp. 2565–2579. doi:10.1088/0022-3700/8/15/018

[9] Colonna, G., Tuttafesta, M., Capitelli, M., and Giordano, D., "Non-Arrhenius NO Formation Rate in One-Dimensional Nozzle Airflow," *Journal of Thermophysics and Heat Transfer*, Vol. 13, No. 3, 1999, pp. 372–375.

[10] Colonna, G., Esposito, F., and Capitelli, M., "The Role of State-Selected Recombination Rates in Supersonic Nozzle Expansion," AIAA Paper 2003-3645, 2003.

[11] Bruno, D., Capitelli, M., Esposito, F., Longo, S., and Minelli, P., "Direct Simulation of Nonequilibrium Kinetics Under Shock Conditions in Nitrogen," *Chemical Physics Letters*, Vol. 360, No. 1, 2002, pp. 31–37.
doi:10.1016/S0009-2614(02)00772-8

[12] Colonna, G., Armenise, I., Bruno, D., and Capitelli, M., "Reduction of State-to-State Kinetic to Macroscopic Models in Hypersonic Flows," *Journal of Thermophysics and Heat Transfer*, Vol. 20, No. 3, 2006, pp. 477–486.
doi:10.2514/1.18377

[13] Josyula, E., and Bailey, W. F., "Vibration-Dissociation Coupling Using Master Equations in Nonequilibrium Hypersonic Blunt-Body Flow," *Journal of Thermophysics and Heat Transfer*, Vol. 15, No. 2, 2001, pp. 157–167.

[14] Josyula, E., and Bailey, W. F., "Vibrational Relaxation and Population Depletion of Nitrogen in Hypersonic Flows," AIAA Paper 2002-0200, 2002.

[15] Josyula, E., and Bailey, W. F., "Vibration-Dissociation Coupling Model for Hypersonic Blunt-Body Flow," *AIAA Journal*, Vol. 41, No. 8, 2003, pp. 1611–1613.

[16] Josyula, E., and Bailey, W. F., "Governing Equations for Weakly Ionized Plasma Flowfield of Aerospace Vehicles," *Journal of Spacecraft and Rockets*, Vol. 40, No. 6, 2003, pp. 845–857.

[17] Josyula, E., and Bailey, W. F., "Nonequilibrium Relaxation in High Speed Flows," AIAA Paper 2004-2468, 2004.

[18] Esposito, F., and Capitelli, M., "Quasiclassical Molecular Dynamic Calculations of Vibrationally and Rotationally State Selected Dissociation Cross Sections: $N + N_2 \rightarrow 3N$," *Chemical Physics Letters*, Vol. 302, No. 1, 1999, pp. 49–54.
doi:10.1016/S0009-2614(99)00099-8

[19] Silva, M. L. D., Guerra, V., and Loureiro, J., "Nonequilibrium Dissociation Processes in Hyperbolic Atmospheric Entries," *Journal of Thermophysics and Heat Transfer*, Vol. 21, No. 2, 2007, pp. 303–310.
doi:10.2514/1.26776

[20] Herzberg, G., *Molecular Spectra and Molecular Structure, 1: Spectra of Diatomic Molecules*, D. Van Nostrand, New York, 1963.

[21] Billing, G. D., and Fisher, E. R., "*VV* and *VT* Rate Coefficients in N_2 by a Quantum-Classical Mode," *Chemical Physics*, Vol. 43, No. 3, 1979, pp. 395–401.
doi:10.1016/0301-0104(79)85207-6

[22] Esposito, F., Capitelli, M., and Gorse, C., "Quasi-Classical Dynamics and Vibrational Kinetics of $N + N_2(v)$ System," *Chemical Physics*, Vol. 257, No. 2, 2000, pp. 193–202.
doi:10.1016/S0301-0104(00)00155-5

[23] Esposito, F., Armenise, I., and Capitelli, M., "N–N_2 State to State Vibrational-Relaxation and Dissociation Rates Based on Quasiclassical Calculation," *Chemical Physics*, Vol. 331, No. 1, 2006, pp. 1–8.
doi:10.1016/j.chemphys.2006.09.035

[24] Capitelli, M., Colonna, G., and Esposito, F., "On the Coupling of Vibrational Relaxation with the Dissociation-Recombination Kinetics: From Dynamic to Aerospace Applications," *Journal of Physical Chemistry A*, Vol. 108, 2004, pp. 8930–8934.
doi:10.1021/jp048847v

[25] Chernyi, G. G., Losev, S. A., Macheret, S. O., and Potapkin, B. V., *Physical and Chemical Processes in Gas Dynamics: Cross Sections and Rate Constants for Physical and Chemical Processes*, Vol. 1, AIAA, Reston, VA, 2002.